Closures for Two-fluid Five-moment Equations for Magnetized Plasmas

Grant Recipient: Utah State University

Final Scientific Report

July 1, 2015 – June 30 2018

Principal Investigator: Jeong-Young Ji
Department of Physics
Utah State University
Logan, UT 84321-4415

November 12, 2018

THE U.S. DEPARTMENT OF ENERGY OFFICE OF FUSION ENERGY SCIENCES AWARD NO. DE-SC0014033

Public Abstract

In the proposed work, we will develop a complete set of closures for two-fluid five-moment equations for magnetized plasmas. Specifically, we propose to obtain explicit formulas for electrons and ions to express heat flow, viscosity, frictional force, and collisional heating in terms of density, and temperature, flow velocity. For this purpose, we solve a set of general moment equations for the relevant closure moments.

An infinite hierarchy of general moment equations is completely equivalent to the original Landau-Fokker-Planck kinetic equation. In the small gyro-period expansion, the parallel components of the general moment equations agree with the moments of the drift-kinetic equation (DKE). The advantages of solving the moment equations include (i) an exact treatment of the collision operator, (ii) closure and transport relations with no flux-surface average, and (iii) a unified form of closures for general collisionality. Practically we solve a truncated set of moment equations and hence must verify the convergence of the solutions by increasing number of moments.

The parallel integral (nonlocal) closures obtained by solving a set of linearized parallel moment equations are useful only when the nonlinear coupling of moments to the temperature and magnetic field gradient terms is negligible. When the nonlinear coupling terms are substantial, we propose a Fourier transform method to solve the parallel moment equations. By Fourier-expanding the magnetic field, we can convert the differential equations of parallel moments to linear algebraic equations for Fourier components of the moments. The convergence of the solutions can be confirmed by increasing the number of Fourier modes. Our preliminary study in axisymmetric circular magnetic geometry with a large aspect ratio shows that (i) the solutions for Fourier modes n=0 and n=1 converge when modes up to n=2 are included in the expansion, and (ii) lower collisionality requires more moments for convergent closures, as in the case of the integral closures. The proposed work will start from this simple magnetic geometry to find general parallel closures and then be generalized to explore a non-circular magnetic field with finite aspect-ratio. With parallel moments known, the perpendicular component of moment closures can be obtained by inverting the generalized cross product operator in the general moment equations.

These efforts will be performed in conjunction with several multi-institutional projects, NIMROD, the Center for Extended MHD Modeling (CEMM), and the Plasma Science and Innovation (PSI) Center.

Products

Journal Publication

1. **J.-Y. Ji** and I. Joseph, "Electron parallel closures for the 3+1 fluid model", Phys. Plasmas **25**, 032117 (2018).

2. **J.-Y. Ji**, G. S. Yun, Y.-S. Na, and E. D. Held, "Electron parallel transport for arbitrary collisionality", Phys. Plasmas **24**, 112121 (2017).

3. **J.-Y. Ji**, H. Q. Lee, and E. D. Held, "Ion parallel closures", Phys. Plasmas **24**, 022127 (2017).

4. **J.-Y. Ji**, G. Park, S. S. Kim, and E. D. Held, "Electron heat flow due to magnetic field fluctuations", Plasma Phys. Control. Fusion **58**, 042001 (2016)

5. **J.-Y. Ji**, S.-K. Kim, E. D. Held, and Y.-S. Na, "Electron parallel closures for various ion charge numbers", Phys. Plasmas **23**, 032124 (2016).

Conference and Workshop Presentations

1. "Parallel closure theory for toroidally confined plasmas", APS-DPP, October 24, 2017, Milwaukee, WI

2. "Updates on development of moment-based closures", NIMROD Team Meeting, August 17, 2017, Boulder. CO.

3. "Electron parallel transport for arbitrary collisionality", EPR Workshop, August 3, 2017, Vancouver, CANADA.

4. "Closures for the 3+1 fluid model", LLNL Seminar, June 14, 2017, Livermore, CA.

5. "Moment approach to plasma kinetic/fluid theory and closures", LLNL Seminar (invited), May 10, 2017, Livermore, CA.

6. "Ion parallel closures for various ions", APS-DPP, November 1, 2016, San Jose, CA.

7. "Parallel closures in an inhomogeneous magnetic field", NIMROD Team Meeting - APS DPP, October 29, 2016, San Jose, CA.

8. "Ion parallel closures", NIMROD Team Meeting, August 9, 2016, Madison, WI.

9. "General moment equation approach to the Coulomb-Milne problem", CEDAR Workshop, June 21, 2016, Santa Fe, NM.

10. "Electron parallel closures and their application to magnetic field fluctuations", EPR Workshop, February 24, 2016, Auburn, AL. 11. "Electron parallel closures", APS-DPP, November 18, 2015, Savannah, GA.

11. "Electron parallel closures for arbitrary ion charge number", NIMROD Team Meeting, August 15, 2015, Tech-X Corporation, Boulder, CO (presented by Eric Held).

Technical Report

The major goal of the project is to develop closures for two-fluid five-moment equations for electron-ion plasmas. The closures are expected to capture kinetic effects and to be valid for arbitrary collisionality and magnetic geometry. In the developed closures, the heat flux density, viscosity tensor, collisional friction force density, and the collisional heating will be expressed in terms of particle density, flow velocity, and temperature of electrons and ions. Here we summarize three major accomplishments achieved in the project.

Integral closures for slab geometry

The closure relations for slab geometry have been developed for arbitrary collisionality. The parallel closures are written as kernel-weighted integrals of parallel thermodynamic drives:

$$n_A(z) = \int dz' K_{AB}(z - z') g_B(z'), \tag{1}$$

where n_A $(A = h, R, \pi)$ are the parallel heat flux $(h_\|)$, viscosity $(\pi_\|)$, and friction $(R_\|)$, and $g_B(B = h, R, \pi)$ are the parallel temperature gradient $(\partial_\| T)$, relative flow between electrons and ions $(V_{\mathrm{ei}\|})$, and rate of strain tensor $(W_\|)$. The kernel functions K_{AB} are explicitly presented for electrons and ions.

For electrons[1], the electron-ion collision effects are considered for different ion charge numbers $Z = 1, 2, \cdots, 10$. Solving the general moment equations and extending to the collisionless limit solutions, fitted kernel functions are obtained and closures are computed. Fig. 1 shows typical behavior of closures due to sinusoidal drives for various Z. For ions[2], the ion-electron collision effects are considered and

[1]J.-Y. Ji, S.-K. Kim, E. D. Held, and Y.-S. Na, "Electron parallel closures for various ion charge numbers", Phys. Plasmas **23**, 032124 (2016).

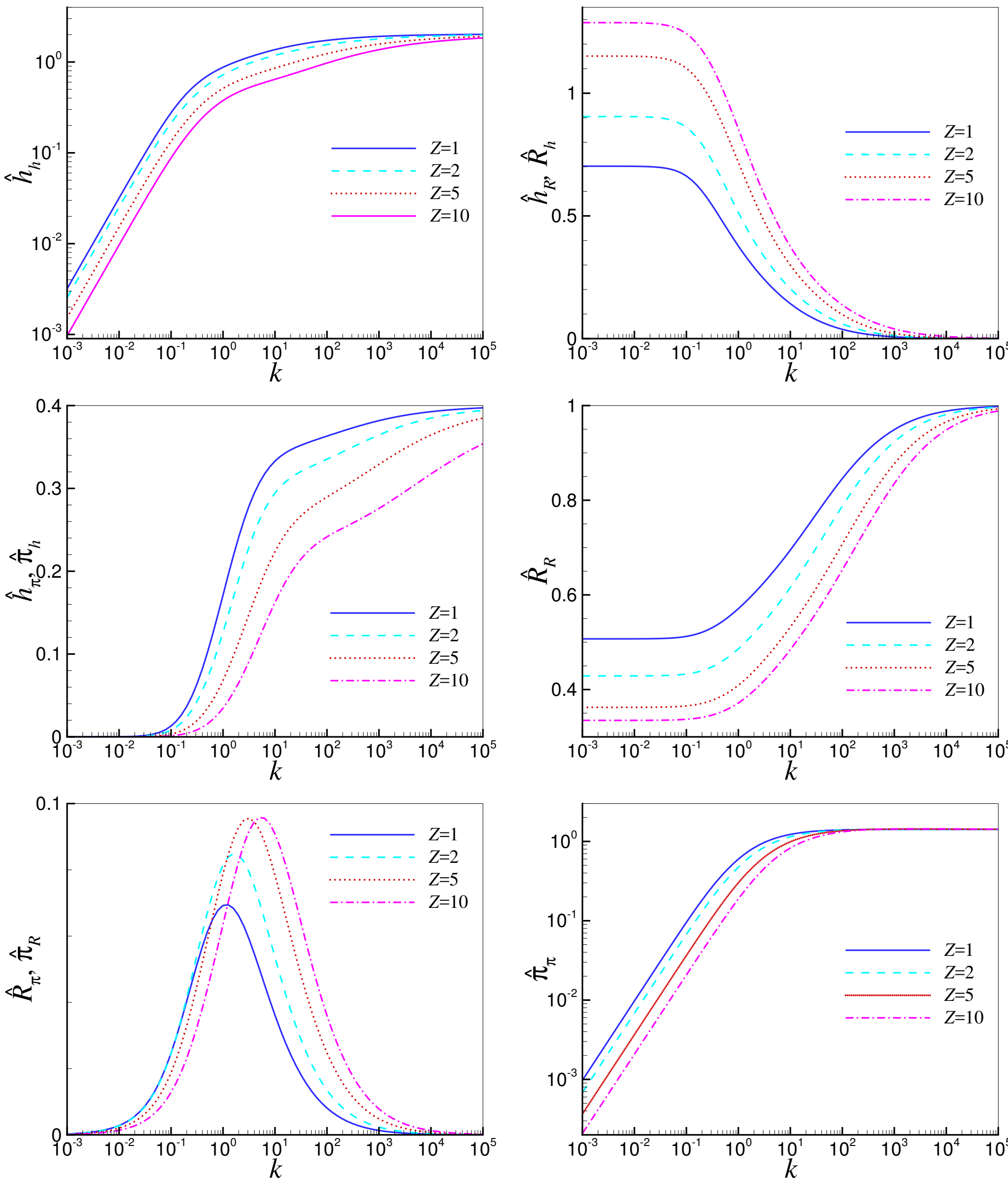

Figure 1: Closures for sinusoidal drives computed from fitted kernels for $Z = 1, 2, 5$, and 10.

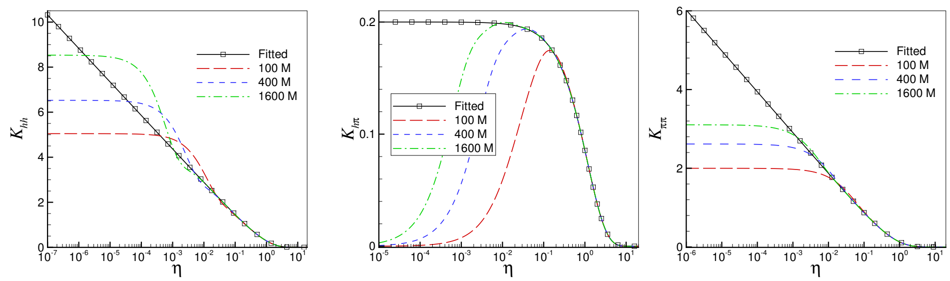

Figure 2: Kernels for $AZ^2 = 1$ and $T_\mathrm{i}/T_\mathrm{e} = 4$. The kernel $K_{\pi h}$ (not shown) is similar to $K_{h\pi}$.

simple fitted kernels are presented to evaluate ion integral closures for electron-to-ion-temperature ratio $T_\mathrm{i}/T_\mathrm{e} \leq 10$, arbitrary collisionality, and arbitrary AZ^2 (ion charge number Z and atomic weight A). Fig. 2 shows typical behavior of kernels for ions.

Applying the results of electron parallel closures, we derive the Spitzer-like transport relations for sinusoidal thermodynamic drives with arbitrary collisionality. One striking result is that the resistivity for low collisionality is much greater than that of Spitzer theory, which elucidates the underlying principle of demonstrated kinetic effects in the literature, providing a natural mechanism for the fast magnetic reconnection[3].

The integral closures for slab geometry are important to verify closures in an inhomogeneous magnetic field. They provide a benchmark for electron and ion closure computations in the large-aspect ratio limit.

Moment-Fourier solver for closures in an inhomogeneous magnetic field

To obtain closures in an inhomogeneous magnetic field, we solve the general parallel moment equations which is equivalent to the drift kinetic equation. With the lowest order distribution being Maxwellian

$$f_0 = \frac{n_0}{\pi^{3/2} v_0^3} e^{-v^2/v_0^2}, \tag{2}$$

we consider the first order drift kinetic equation to determine $\bar{f}_1$,

$$v_\parallel \mathbf{b} \cdot \nabla \bar{f}_1 + \mathbf{v}_\mathrm{d} \cdot \nabla \bar{f}_0 + q v_\parallel E_\parallel \frac{\partial \bar{f}_0}{\partial w} = C(\bar{f}_1). \tag{3}$$

[2]J.-Y. Ji, H. Q. Lee, and E. D. Held, Phys. Plasmas **24,** 022127 (2017) “Ion parallel closures”.

[3]J.-Y. Ji, G. S. Yun, Y.-S. Na, and E. D. Held, “Electron parallel transport for arbitrary collisionality”, Phys. Plasmas **24**, 112121 (2017).

where

$$\mathbf{v}_\mathrm{d} = \frac{1}{\Omega}\mathbf{b} \times [(v_\parallel^2 + \frac{1}{2}v_\perp^2)\frac{\nabla B}{B}]. \tag{4}$$

For gyro-averaged distribution function, we expand $\bar{f}$ (hereafter the subscript 1 will be omitted)

$$\bar{f} = \hat{f}_0 \sum_{l,k} \hat{P}^{lk} n^{lk} \tag{5}$$

with

$$\hat{P}^{lk} = \frac{1}{\sqrt{\bar{\sigma}_{lk}}} P_l(v_\parallel/v) L_k^{(l+1/2)}(s^2),$$

where P_l is a Legedre polynomial, $L_k^{(l+1/2)}$ is an associated Laguerre (Sonine) polynomial and normalization constants are

$$\bar{\sigma}_{lk} = \bar{\sigma}_l \lambda_{lk},\ \bar{\sigma}_l = \frac{1}{2l+1},\ \lambda_{lk} = \frac{(l+k+1/2)!}{k!(1/2)!}. \tag{6}$$

The (l,p) moment equation can be obtained by multiplying $\hat{P}^{lp}$ to Eq. (3) and integrating over velocity variable $\mathbf{v}$. A system of the moment equations can be written in matrix form

$$[\psi]\left[\partial_\parallel N\right] + [\psi_B]\left(\partial_\parallel \ln B\right)[N] = \frac{1}{\lambda_\mathrm{C}}[c][N] + \frac{1}{v_0}\left[g_\parallel\right] + \frac{B_0 \partial_\parallel \ln B}{B}\left\{[g_p]\,p_\star + [g_T]\,T_\star\right\}. \tag{7}$$

For the axisymmetric magnetic field (26), using $\partial_\parallel = \mathbf{b}\cdot\nabla = (B^\theta/B)\partial_\theta$ where θ is the poloidal angle, we rewrite the moment equation as

$$[\psi]\,\partial_\theta\,[n] + [\psi_B]\,(\partial_\theta \ln B)\,[n] = \hat{\nu}_0\,[c]\,[n] + [g_a] + \epsilon \sin\theta \left\{[g_p]\,p_\star + [g_T]\,T_\star\right\}, \tag{8}$$

where the collisionality $\hat{\nu}_0$ and inverse collisionality K_0 are given by

$$\hat{\nu}_0 = \frac{B}{B^\theta \lambda_\mathrm{C}},\ K_0 = \frac{1}{\hat{\nu}_0}.$$

Here nonvanishing parallel drives for a species are

$$\begin{aligned}
g_{ah}^{11} &= \frac{\sqrt{5}}{2}\frac{\partial}{\partial\theta} n_{a0}\hat{T}_a, \\
g_{\mathrm{e}R}^{1k} &= \frac{B}{B^\theta}\frac{1}{v_{\mathrm{e}0}\tau_{\mathrm{ee}}}\sqrt{2} Z a_{\mathrm{ei}}^{1k0} n_{\mathrm{e}0}\hat{V}_{\mathrm{ei}}, \\
g_{a\pi}^{20} &= -\frac{2}{\sqrt{3}}\left[\partial_\theta + \frac{1}{2}(\partial_\theta \ln B)\right] n_{a0}\hat{V}_a,
\end{aligned}$$

with dimensionless variables defined as

$$\hat{T}_a = \frac{T_a}{T_{a0}},\ \hat{V}_a = \frac{V_\|}{v_{Ta}},\ \hat{V}_{\rm ei} = \frac{V_{\rm e\|} - V_{\rm i\|}}{v_{T\rm e}}.$$

Nonvanishing coefficients for radial gradients

$$\begin{aligned} p_\star &= n_0\rho_0 I\frac{d\ln p_0}{d\psi}, \\ T_\star &= n_0\rho_0 I\frac{d\ln T_0}{d\psi}, \end{aligned}$$

are

$$g_p^{20} = \frac{1}{\sqrt{12}},\ g_T^{02} = \sqrt{\frac{10}{3}},\ g_T^{20} = \frac{1}{\sqrt{12}},\ g_T^{21} = -\sqrt{\frac{7}{24}}. \tag{9}$$

Now Fourier expanding all physical variables as

$$[n] = \left[n_0^+\right] + \sum_{m=1}^{\texttt{nfo}}\left(\left[n_m^+\right]\cos m\theta + \left[n_m^-\right]\sin m\theta\right), \tag{10}$$

the system of differential equations (8) becomes a system of algebraic equations for Fourier coefficients of moments with the replacement

$$[\psi]\,X(\theta)\,[n(\theta)] \to [\psi]\otimes[X]\,[n]\,,\ X = \frac{d}{d\theta},\ \cos m\theta,\ \sin m\theta,$$

or in component form,

$$\sum_{lk}\psi^{jp,lk}X(\theta)n^{lk} \to \sum_{lkq}\psi^{jp,lk}X_{mq}n_q^{lk}.$$

With the notation $(0,1^-,1^+,2^-,2^+,\cdots) \to$ `subscript` $(1,2,3,4,5,\cdots)$ and $(l,k)\to$ `superscript` A, the solution is

$$\begin{pmatrix} n_1^A \\ n_2^A \\ n_3^A \\ n_4^A \end{pmatrix} = \sum_{B=h,R,\pi}\begin{bmatrix} \chi_{11}^{AB} & \chi_{12}^{AB} & \chi_{13}^{AB} & \chi_{14}^{AB} \\ \chi_{21}^{AB} & \chi_{22}^{AB} & \chi_{23}^{AB} & \chi_{24}^{AB} \\ \chi_{31}^{AB} & \chi_{32}^{AB} & \chi_{33}^{AB} & \chi_{34}^{AB} \\ \chi_{41}^{AB} & \chi_{42}^{AB} & \chi_{43}^{AB} & \chi_{44}^{AB} \end{bmatrix}\begin{pmatrix} g_1^B \\ g_2^B \\ g_3^B \\ g_4^B \end{pmatrix} + \sum_{\beta=p,T}\begin{pmatrix} \chi_1^{A\beta} \\ \chi_2^{A\beta} \\ \chi_3^{A\beta} \\ \chi_4^{A\beta} \end{pmatrix}\frac{d\beta_0}{d\psi}, \tag{11}$$

where $A,B = h,R,\pi$ and $\beta = p,T$. It can be explicitly written as

$$(h) = \left[\chi^{hh}\right](T) + \left[\chi^{hR}\right](u_{\rm ei}) + \left[\chi^{h\pi}\right](u) + \left(\chi^{hp}\right)\frac{dp_0}{d\psi} + \left(\chi^{hT}\right)\frac{dT_0}{d\psi}, \tag{12}$$

$$(R) = \left[\chi^{Rh}\right](T) + \left[\chi^{RR}\right](u_{\rm ei}) + \left[\chi^{R\pi}\right](u) + \left(\chi^{Rp}\right)\frac{dp_0}{d\psi} + \left(\chi^{RT}\right)\frac{dT_0}{d\psi}, \tag{13}$$

$$(\pi) = \left[\chi^{\pi h}\right](T) + \left[\chi^{\pi R}\right](u_{\rm ei}) + \left[\chi^{\pi\pi}\right](u) + \left(\chi^{\pi p}\right)\frac{dp_0}{d\psi} + \left(\chi^{\pi T}\right)\frac{dT_0}{d\psi}, \tag{14}$$

where (h), (R), (π), (T), (u_{ei}), and (u) are the corresponding column vectors of Fourier coefficients, $\left[\chi^{AB}\right]$ $(A, B = h, R, \pi)$ are closure matrices connecting closures to parallel drives, and $\left(\chi^{AB}\right)$ $(A = h, R, \pi, \ B = p, T)$ are closure column vectors connecting closures to radial drives.

The Moment-Fourier solver has been written in Fortran to solve the algebraic system for arbitrary aspect ratio and collisionality. Due to restriction of exact arithmetic in computing collision matrix, the current maximum moments are 25600 $(lp = 160 \times 160)$. This number can be increased through exact arithmetic of the Mathematica software. The number of Fourier modes can be increased arbitrarily as the computation capacity is available. The Fourier expansion of the magnetic field is extended to compute closures for an arbitrary order in the input file. The code has been tested with simple axisymmetric magnetic geometry with nested flux surfaces. The convergence property with increasing the number of moments and Fourier modes has been investigated. A larger number of moments are required for lower collisionality. The $N = 6400$ moments yield convergent closures for the Knudsen number $K_0 = 500$ for Fourier mode number $n = 2$. Convergent closures for larger K_0 and n require more moments. The closures are expressed with Fourier modes in response to Fourier expanded thermodynamic drives.

In Figs. 3 and 4, convergence with increasing Fourier modes is verified. Figure 3 shows convergent results for $\epsilon = 0.1$ are obtained with $\texttt{nfo} = 2$ in Eq. (10). Figure 4 shows convergent results for $\epsilon = 0.5$ with $\texttt{nfo} = 6$.

Convergence with increasing moments is also verified. Figure 5 shows convergent closures due to radial derivative drives are achieved by 20×20 moment calculations. Figure 6 shows convergent closures due to $\cos\theta$ parallel drives with 40×40 calculations. Finally, Fig. 7 shows convergent closures due to $\sin 3\theta$ parallel drives with 40×40 moment calculations.

DKE-Fourier solver for closures in an inhomogeneous magnetic field

Since the Fourier-moment solver is impractical in the collisionless limit, we solve a reduced kinetic equation to obtain the collisionless-limit closures. We adopt a Krook-type collision operator

$$C(f) = -\nu(f - f^{\mathrm{M}}) = -\nu f^{\mathrm{N}}$$

which conserves the particle number, momentum, and energy, where f^{M} and f^{N} are the Maxwellian and non-Maxwellian distributions, respectively. A big advantage of using the model operator is that we can find the analytical solution in the configuration space. Since the details of the collision operator does not affect the final results in the collisionless limit, the model operator will result in the same solution obtained from the Landau-Fokker-Planck operator. In solving the kinetic

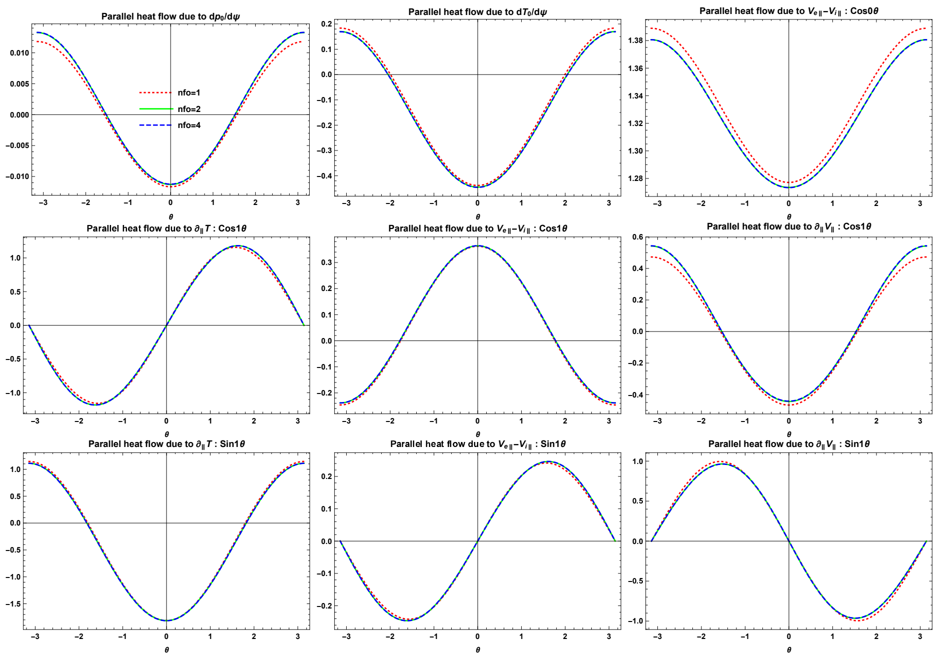

Figure 3: Convergence with increasing Fourier modes for $\epsilon = 0.5$ and $K_0 = 10$.

equation, one crucial step is to remove the fluid equations to be closed[4]. The kinetic equation for $F = f^{\mathrm{N}}/\hat{f}_0$ is written as

$$\left(s_{\|}\frac{\partial}{\partial\theta} + \frac{\alpha\nu}{v_0}\right)F = \left[\left(s^2 - \frac{3}{2}\right)\frac{2}{3}\partial_\theta^{0+}\hat{h} + s_{\|}\partial_\theta^{1+}\hat{\pi}\right] + \frac{\alpha}{v_0}G_{\mathrm{M}}, \tag{15}$$

where $\hat{f}_0 = \pi^{-3/2}v_0^{-3}\exp(-s^2)$, $s = v/v_0$, $v_0 = \sqrt{2T_0/m}$, $s_{\|} = \pm\sqrt{\hat{w} - \hat{\mu}\hat{B}}$, $\hat{w} = s^2$, $\hat{\mu} = \sqrt{s^2 - s_{\|}^2}/\hat{B}$, $\hat{B} = B/B_0$, $\hat{h} = h_{\|}/v_0T_0$ (heat flow) and $\hat{\pi} = \pi_{\|}/T_0$ (viscosity), θ is the poloidal angle, $\alpha = d\theta/d\ell = B^\theta/B$, ℓ is the arclength along a field line, and G_{M} involves the thermodynamic drives $dp_0/d\psi,\ dT_0/d\psi,\ \mathbf{b}\cdot\nabla T$, and $W_{\|}$ (the rate of strain tensor). Once the solution F has been obtained in terms of $\hat{h}$, $\hat{\pi}$, and G_{M}, taking $\hat{h}$ and $\hat{\pi}$ moments of $f^{\mathrm{N}} = \hat{f}_0F$ will produce a coupled system of integro-differential equations for $\hat{h}$ and $\hat{\pi}$.

To solve the integro-differential equations we expand $H = \hat{h},\ \hat{\pi},\ u$, and T in

[4]J.-Y. Ji, E. D. Held, and H. Jhang, Phys. Plasmas **20,** 082121 (2013) "Linearly exact parallel closures for slab geometry".

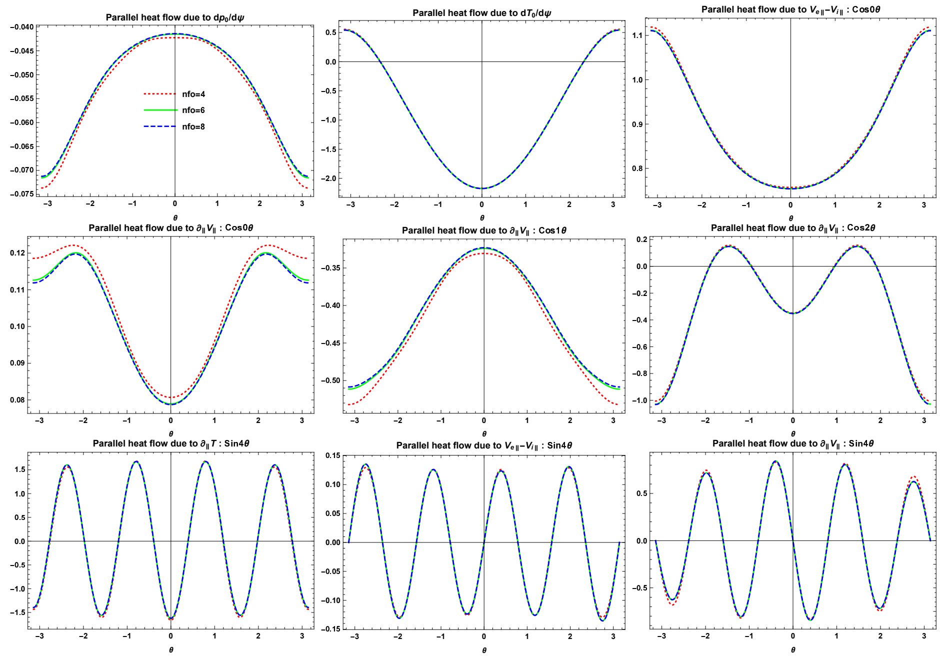

Figure 4: Convergence with increasing Fourier modes for $\epsilon = 0.1$ and $K_0 = 10$.

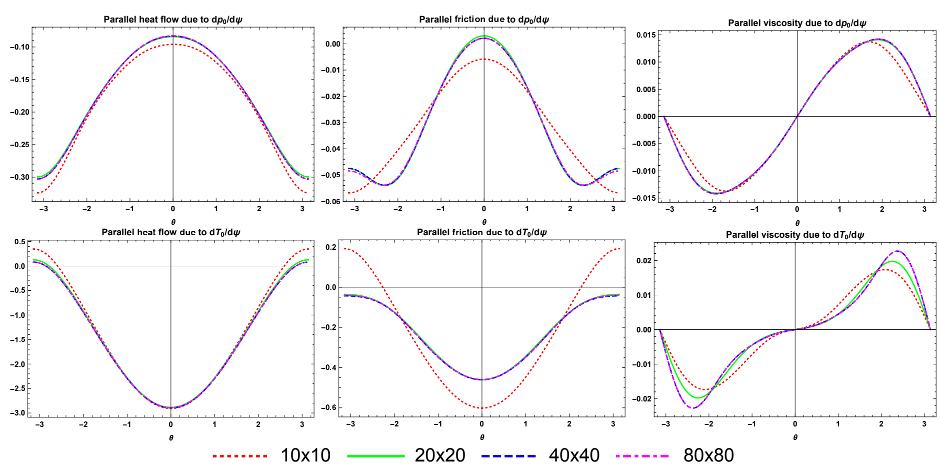

Figure 5: Closures responding to radial gradient drives. Convergence with increasing moments for $\epsilon = 0.5$ and $K_0 = 100$.

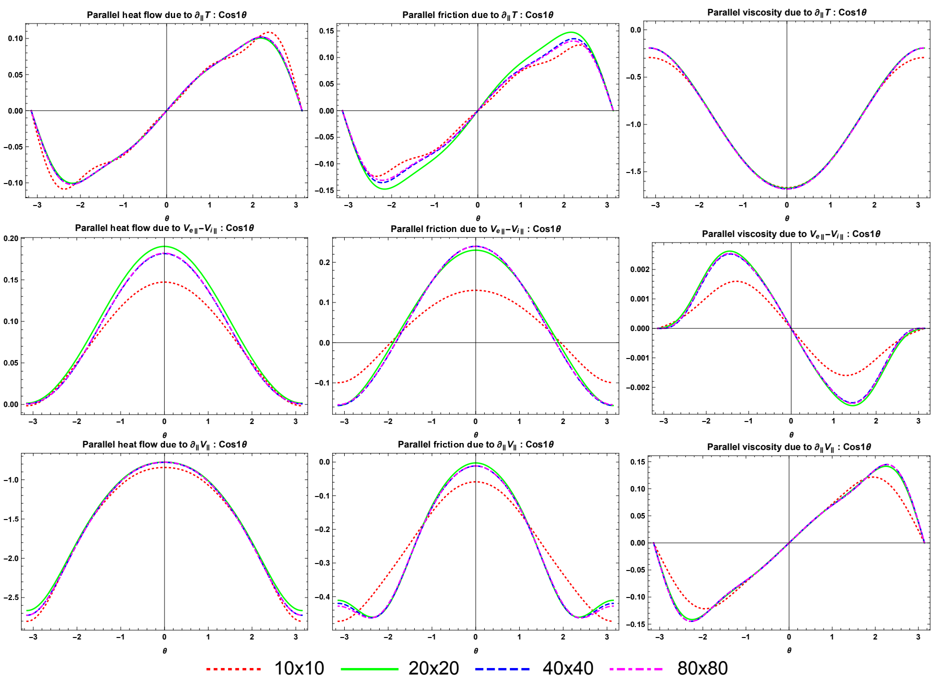

Figure 6: Closures responding to $\cos\theta$ parallel drives. Convergence with increasing moments for $\epsilon = 0.5$ and $K_0 = 100$.

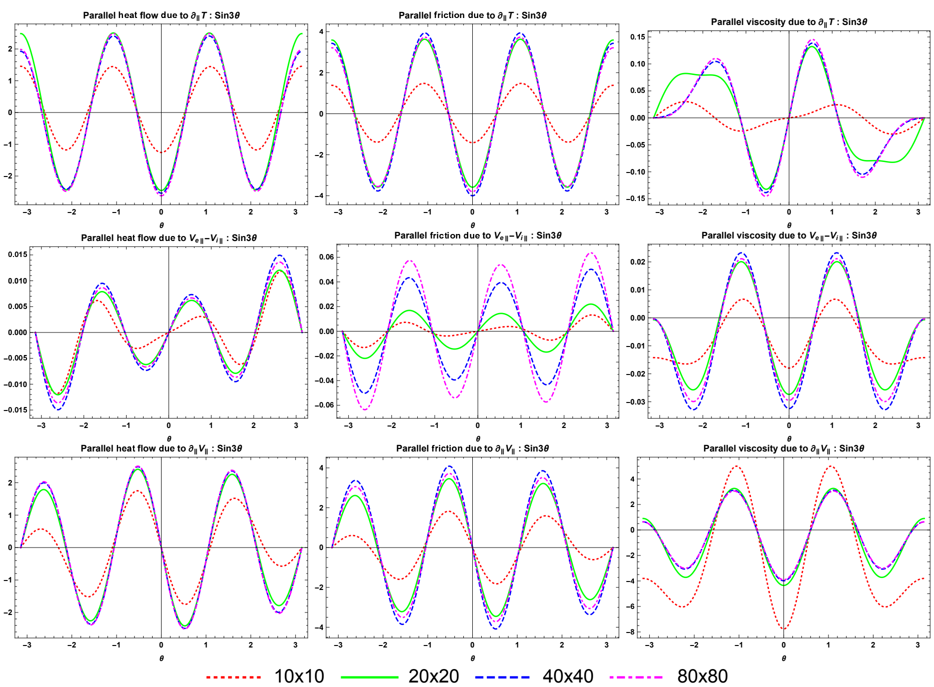

Figure 7: Closures responding to $\sin 3\theta$ parallel drives. Convergence with increasing moments for $\epsilon = 0.5$ and $K_0 = 100$.

Fourier series

$$H(\theta) = H_0 + \sum_{j=1}^{J}(H_{j+}\cos j\theta + H_{j-}\sin j\theta). \tag{16}$$

Then, for a single term of the right hand side, Eq. (15) becomes

$$\left(s_\parallel \frac{\partial}{\partial\theta} + \frac{\alpha\nu}{v_0}\right)F_\sigma = G_\sigma(\theta) \tag{17}$$

where $\sigma = \pm 1$ stands for $\pm s_\parallel > 0$ and G_σ is a single Fourier term multiplied by velocity polynomials, $s_\parallel$ and/or $d\ln\hat{B}/d\theta$. Although one can Fourier-expand $s_\parallel$ and F_σ to convert the differential equation (15) to a system of algebraic equations, the Fourier expansion of $s_\parallel$ is very inefficient due to its C^1-discontinuity. The general solution is of Eq. (17) is given by the kernel-weighted integral with the kernel defined by

$$K_+(\theta_1,\theta_2) = \int_{\theta_1}^{\theta_2}\frac{d\theta}{\sqrt{\hat{w}-\hat{\mu}\hat{B}(\theta)}}. \tag{18}$$

In the passing particle regime of the velocity space, for $-\pi \le \theta \le \pi$, the solution is

$$F_+(\theta) = \frac{\left(\int_{-\pi}^{\theta} e^{-\frac{\alpha\nu}{v_0}\hat{K}_+(\phi,\theta)} + e^{-\frac{\alpha\nu}{v_0}\hat{K}_+(-\pi,\pi)}\int_{\theta}^{\pi} e^{-\frac{\alpha\nu}{v_0}\hat{K}_+(\phi,\theta)}\right)\frac{+\alpha}{|s_\parallel(\phi)|}G_+(\phi)d\phi}{1-e^{-\frac{\alpha\nu}{v_0}\hat{K}_+(-\pi,\pi)}}, \tag{19}$$

$$F_-(\theta) = \frac{\left(e^{-\frac{\alpha\nu}{v_0}\hat{K}_+(-\pi,\pi)}\int_{-\pi}^{\theta} e^{-\frac{\alpha\nu}{v_0}\hat{K}_+(\theta,\phi)} + \int_{\theta}^{\pi} e^{-\frac{\alpha\nu}{v_0}\hat{K}_+(\theta,\phi)}\right)\frac{+\alpha}{|s_\parallel(\phi)|}G_-(\phi)d\phi}{1-e^{-\frac{\alpha\nu}{v_0}\hat{K}_+(-\pi,\pi)}}. \tag{20}$$

In the trapped particle regime, for $-\theta_\mathrm{b} \le \theta \le \theta_\mathrm{b}$, the solution is

$$F_+(\theta) = e^{-\frac{\alpha\nu}{v_0}\hat{K}_+(-\theta_\mathrm{b},\theta)}F(-\theta_\mathrm{b}) + \int_{-\theta_\mathrm{b}}^{\theta} e^{-\frac{\alpha\nu}{v_0}\hat{K}_+(\phi,\theta)}\frac{\alpha}{|s_\parallel(\phi)|}G_{0+}(\phi)d\phi, \tag{21}$$

$$F_-(\theta) = e^{-\frac{\alpha\nu}{v_0}\hat{K}_+(\theta,\theta_\mathrm{b})}F(\theta_\mathrm{b}) + \int_{\theta}^{\theta_\mathrm{b}} e^{-\frac{\alpha\nu}{v_0}\hat{K}_+(\theta,\phi)}\frac{\alpha}{|s_\parallel(\phi)|}G_{0-}(\phi)d\phi, \tag{22}$$

where

$$F(\theta_\mathrm{b}) = \frac{\int_{-\theta_\mathrm{b}}^{\theta_\mathrm{b}}\left[e^{-\beta}e^{-\beta_+(-\theta_\mathrm{b},\phi)}G_{0-}(\phi) + e^{-\beta_+(\phi,\theta_\mathrm{b})}G_{0+}(\phi)\right]\frac{\alpha}{|s_\parallel(\phi)|}d\phi}{1-e^{-2\beta}}, \tag{23}$$

$$F(-\theta_\mathrm{b}) = \frac{\int_{-\theta_\mathrm{b}}^{\theta_\mathrm{b}}\left[e^{-\beta}e^{-\beta_+(\phi,\theta_\mathrm{b})}G_{0+}(\phi) + e^{-\beta_+(-\theta_\mathrm{b},\phi)}G_{0-}(\phi)\right]\frac{\alpha}{|s_\parallel(\phi)|}d\phi}{1-e^{-2\beta}}, \tag{24}$$

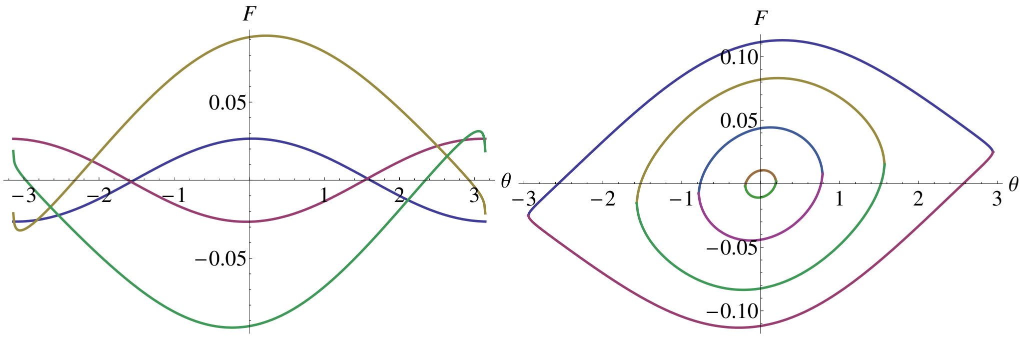

Figure 8: Typical solutions $F_{\pm}^{\text{passing}}$ (left) and $F_{\pm}^{\text{trapped}}$ (right) for various $\hat{w}$ and $\hat{\mu}$ responding to a sinusoidal drive.

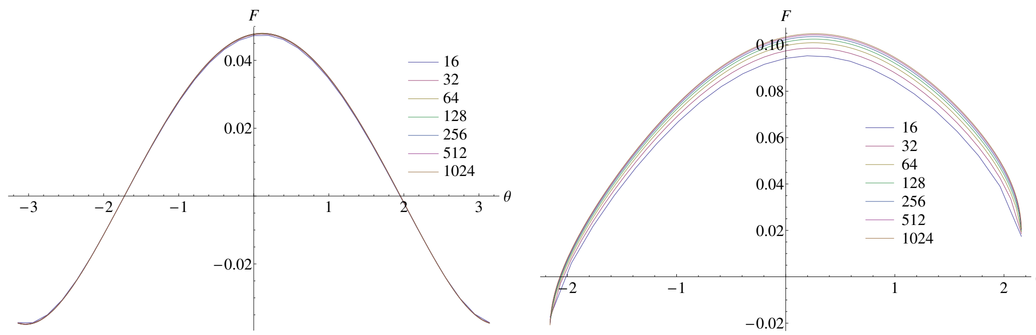

Figure 9: Convergence of increasing the θ resolution for passing (left) and trapped (right) regime solutions.

and

$$\theta_{\rm b} = \cos^{-1}\left[\frac{1}{\epsilon}(\frac{\hat{\mu}}{\hat{w}} - 1)\right]. \tag{25}$$

The $\hat{w}$ grid is chosen to perform the Gauss-Laguerre integration and the $\hat{\mu}$ grid is adaptively chosen for high precision trapezoidal integration. For given $\hat{w}$ and $\hat{\mu}$, the DKE-Fourier solver has computed the solution for the various Knudsen numbers $k = \alpha\nu/v_0$, and the inverse aspect ratios ϵ with a standard model of magnetic field

$$B(\theta) = \frac{B_0}{1 + \epsilon\cos\theta}. \tag{26}$$

Figure 8 shows typical passing and trapped regime solutions. Figure 9 shows the convergence of the FDM solution as the θ grid resolution increases. While the Krook operator is a crude approximation of the exact Coulomb operator, the

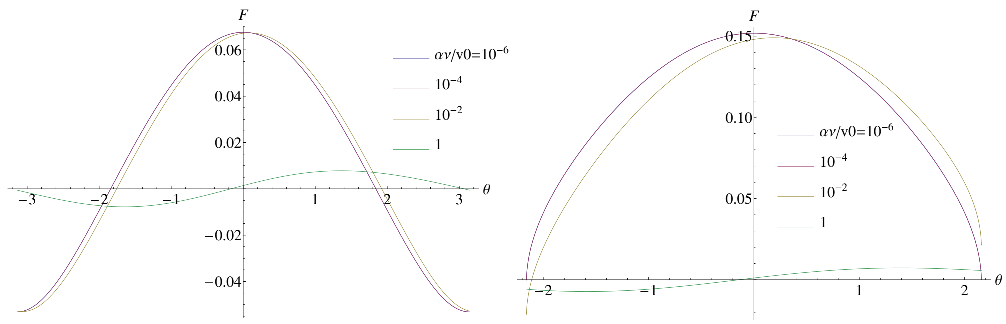

Figure 10: Passing (left) and trapped (right) solutions as decreasing collisionality.

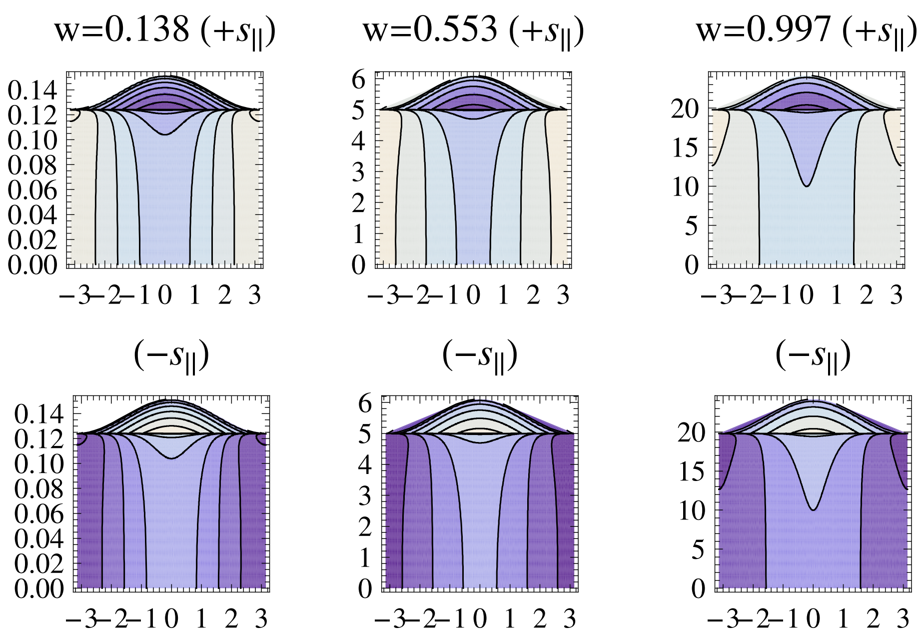

Figure 11: $F_{\pm}(\theta, \hat{\mu})$ for $\alpha\nu/v_0 = 10^{-6}$ with various $\hat{w}$ values. $\pm s_{\|}$ stands for $\pm s_{\|} > 0$.

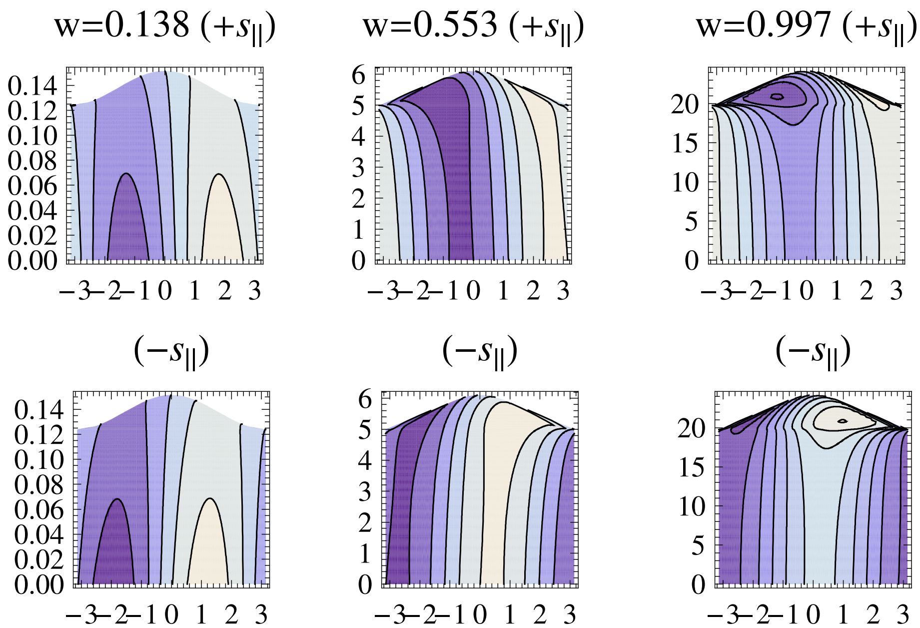

Figure 12: $F_{\pm}(\theta, \hat{\mu})$ for $\alpha\nu/v_0 = 1$ with various $\hat{w}$ values. $\pm s_{||}$ stands for $\pm s_{||} > 0$.

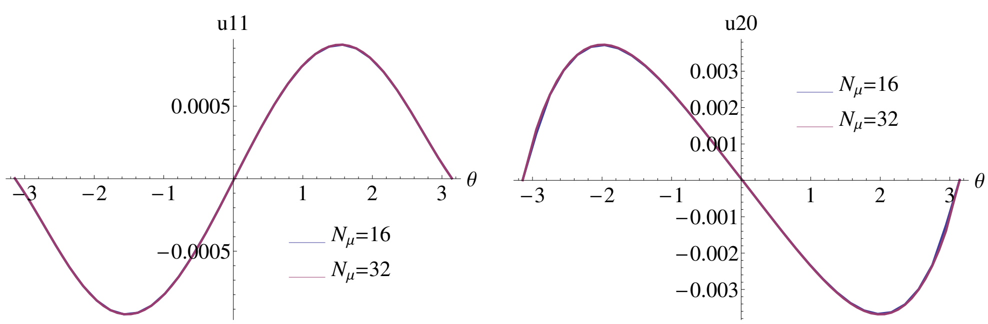

Figure 13: Heat flow (u11, left) and viscosity (u20, right) responding to $dp_0/d\psi$

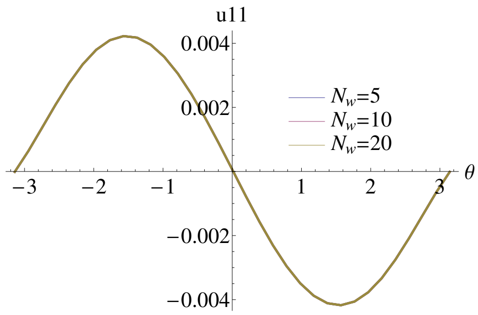

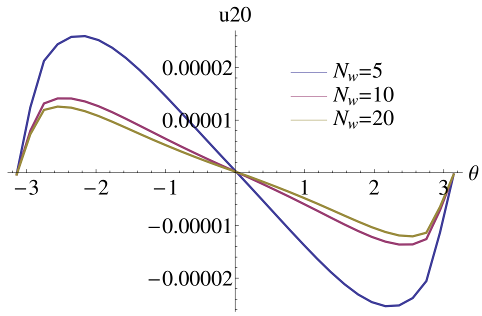

Figure 14: Heat flow (u11, left) and viscosity (u20, right) responding to $dT_0/d\psi$

solution becomes the one of exact operator in the collisionless limit. Figure 10 shows that the solution converges in the collisionless limit. Figures 11 and 12 show distribution functions in the θ-$\hat{\mu}$ plane. Finally, Figs. 13 and 14 show the heat flow (u11) and viscosity (u20) driven by $dp_0/d\psi$ and $dT_0/d\psi$, respectively.

Conclusion

Methods of obtaining closures for two-fluid five-moment equations for magnetized plasmas have been developed. For collisional to nearly collisionless plasmas, the Moment-Fourier solver provides accurate closure relations for arbitrary aspect ratios. In the collisionless limit, the DKE-Fourier solver may provide the collisionless solution when the numerical quadrature scheme for moment integration over velocity variable is precise enough to capture the collisionless response. The 160×160 moment calculations produce convergent closures for $K_0 \lesssim 500$, a nearly collisionless regime. In this regime, the deviation of the Moment-Fourier closures from the collisionless closures is less than 10% and hence $K_0 = 500$ closures are good approximations for the collisionless response. Furthermore, an effort of analytically resolving the high-precision to capture collisionless response from the DKE-Fourier solver will be continued.

Instead of solving the Moment-Fourier solver to compute closures in an existing fluid code such as NIMROD, we plan to provide closure matrices $\left[\chi^{AB}\right]$ and column vectors $\left(\chi^{AB}\right)$ in terms of explicit functions of K_0 and ϵ. The explicit formulas can be conveniently used in fluid simulations and in theoretical investigations of transport relations. All analytical work and computational results accomplished in this Project are to be published in the near future.